Chain Retraction Potential in a Fixed Entanglement Network

Sachin Shanbhag and Ronald G. Larson*

Department of Chemical Engineering, University of Michigan, Ann Arbor, Michigan 48109-2136, USA

(Received 20 September 2004; published 23 February 2005)

When a chain, tethered at one end, is immersed in a fixed entanglement network, the mobile tip of the chain encounters an entropic potential barrier that penalizes deep fluctuations needed to bring the tip close to the tethering point. Using the tube model, Doi and Kuzuu [J. Polym. Sci., Polym. Lett. Ed. **18**, 775 (1980)] estimated that this potential, which is crucial to describe the rheology of branched polymers in fixed networks and melts, has a quadratic form with a prefactor $\nu = 1.5$. Later calculations based on regular lattices indicated that the potential is nonquadratic, and its steepness depends on the lattice coordination number. In this Letter, we analyze the primitive paths obtained using the bond-fluctuation model for chains with up to 12.5 entanglements. Our simulations confirm a quadratic form for the potential with a prefactor close to the Doi-Kuzuu value, $\nu \approx 1.5$.

DOI: 10.1103/PhysRevLett.94.076001 PACS numbers: 83.10.Kn, 61.25.–f, 83.10.Rs

Introduction.—The rheology of branched polymer melts is of enormous scientific and commercial interest. Relaxation in these polymers is primarily controlled by the process of contour-length fluctuation, where an arm tethered at one end by the branch point renews its conformation by a series of ''inward'' and ''outward'' fluctuations along its contour within the hypothetical ''tube'' that confines its lateral motion. The arm pays a stiff entropic penalty for large inward excursions since they necessitate the formation of large unentangled loops, making such configurations exponentially rare. The retraction of the tip of the arm towards the branch point along its contour can be considered as an activated process and may be mapped approximately to the problem of a Brownian particle diffusing over an entropic barrier. For a chain exploring its conformations in a fixed entanglement network, this entropic potential can be constructed by summing up the contributions of the rubber elastic and the end-tension terms [1–3]. If we define the primitive path corresponding to a given conformation of a polymer chain immersed in a network of obstacles as the shortest path connecting the two ends of the polymer chain subject to the topological constraints imposed by the obstacles [4], then the entropic potential can be derived, under the simplifying assumption of a straight tube as

$$\frac{U(L) - U(L_{\mathrm{eq}})}{k_B T} = \nu \frac{L_{\mathrm{eq}}}{a}\left(1 - \frac{L}{L_{\mathrm{eq}}}\right)^2 \qquad (1)$$

where L is the length of the primitive path which fluctuates around a equilibrium value L_{eq} according to the quadratic potential above, a is the average length of a primitive-path step, and $\nu = 3/2$ is a constant whose value arises from tube model [1].

Lattice calculations based on primitive-path analysis of a chain in a regular lattice of fixed obstacles [5–8] indicate that while a quadratic describes shallow fluctuations around L_{eq} quite well, the potential experienced by a chain end for deep fluctuations is not as steep as that specified by (1). The shape and depth of the potential are found to depend on details of the lattice, such as the coordination number z and the ratio of the lattice spacing c, to the random walk step length b. For example, 2D and 3D lattices have been found to have deviations from a quadratic potential, and the quadratic part of the potential has a prefactor given by $\nu = z(z-2)/8(z-1)$ [9,10], when $c/b = 1$. This potential agrees with the classical potential with $\nu = 1.5$, if z is arbitrarily set to $z = 13$. Likewise, for deep fluctuations on a regular 3D cubic lattice the value of ν varies from 3.403 to 0.850 [8], as c/b increases from 1 to 64, with $\nu \approx 1.5$ around $c/b \approx 7$. Unfortunately, for branched polymers, many important rheological properties are governed by these deep fluctuations, for which the primitive-path length $L \approx a$, where the disagreement between the traditional potential given by Eq. (1) with $\nu = 1.5$ and predictions of the lattice models is most severe. Currently, despite criticism, Eq. (1) continues to be widely used because of the absence of a superior alternative and is a vital component of nearly all theories describing the dynamics of branched polymers in *melts*, where the quadratic potential derived for a fixed network is modified to include the effect of simultaneous relaxation of matrix chains by constraint release [11–13]. Obviously, if we do not know what potential should be used for a fixed entanglement network, we cannot use experimental data to assess the degree to which constraint release modifies that potential.

In this Letter, we calculate the fluctuation potential directly from the primitive-path statistics using the bond-fluctuation model [14] (BFM), modified by Shaffer [15,16]. The BFM has been shown to reproduce important features of entangled linear [15,16] and star [17] polymers. We also adapt the procedure described in [18] for computing the primitive paths of chains in an off-lattice molecular dynamics (MD) simulation, to the lattice-based BFM. We generate a statistical distribution of primitive paths from which the entropic potential is inferred. Moreover, our method for constructing the potential is general, and is

 © 2005 The American Physical Society

applicable to real space simulations, once computer power becomes adequate to carry out the large number of realizations required for accurate calculation of the potential to be obtained.

Simulation method.—In the modified BFM [15], polymer beads are placed on a simple cubic lattice, where *excluded volume* interactions are implemented by allowing only a single bead to occupy a lattice site at any given instant. *Chain connectivity* is maintained by restricting the lengths of bonds connecting neighboring beads to the set $\{1, \sqrt{2}, \sqrt{3}\}$ in units of lattice spacing. Because of the geometry of the lattice, *chain uncrossability* is enforced by forbidding the intersection of the midpoints of the bonds. To execute chain motion, we attempt to move a randomly selected bead to one of the six nearest-neighbor sites. A move is accepted if it does not violate the excluded volume, chain connectivity and chain uncrossability conditions.

To initialize, chains are simultaneously grown on the lattice with bond types $\{1, \sqrt{2}, \sqrt{3}\}$ chosen with probabilities $\{3/13, 6/13, 4/13\}$, respectively. During the growth phase, excluded volume is enforced, but intersection of chains is permitted.

After generating the chains, the chain uncrossability condition can be ''switched off'' at first, allowing the bonds to cross each other freely in the first phase of the equilibration. Since the global structural features of crossing and noncrossing chains are indistinguishable from each other [15], this procedure speeds up the computation time required to fully equilibrate the chains. In our simulations we monitored the decorrelation of the end-to-end vector $\langle \mathbf{P}(t) \rangle = \langle \mathbf{R}(t) \cdot \mathbf{R}(0) \rangle / \langle \mathbf{R}^2(0) \rangle$. The chains were permitted to pass through each other while $1 > \langle \mathbf{P}(t) \rangle > 0.3$, after which the uncrossability condition was ''switched on''. The equilibration was carried on until $\langle \mathbf{P}(t) \rangle = 0.05$.

It has been found that a bead density of $\rho = 0.5$ [16,17,19], which is the value we use in all the simulations in this Letter, reproduces melt dynamics quite well. At lower densities, $\rho < 0.25$, the system exhibits dilute good-solvent behavior ($\langle R^2 \rangle \sim N^{1.2}$). Densities up to $\rho = 0.7$ [20] have been accessed using the BFM. It may be noted that while the BFM is not completely ergodic, it has been found [16] that the fraction of immobile configurations for 3D simulations is negligible and the effect on ensemble averages is expected to be unimportant.

In the simulations, N_p polymer chains, each composed of N beads, were simulated in a box of size $L_{\text{box}} \times L_{\text{box}} \times L_{\text{box}}$, with periodic boundary conditions. In this paper, all the lengths are reported in units of the lattice spacing. One Monte Carlo step consists of $N \times N_p$ attempted bead moves. Simulation parameters and results are summarized in Table I.

Following the method of [18] to compute the primitive paths of the equilibrated polymers, we anchor the ends of all the chains in the system and permit their internal beads to move. During this phase we switch off *intramolecular* excluded volume interactions while preserving chain uncrossability and *intermolecular* excluded volume interactions. We ''anneal'' all chains in the system simultaneously, gradually restricting the tolerance with which moves that increase the contour length are accepted, according to the probability, $p_{\text{acc}}(t) = \exp[-A \Delta L (t/\tau_{\text{anneal}})^2]$, where ΔL is the change in chain contour length due to the trial move, and we use $\tau_{\text{anneal}} \approx 10 \times \tau_{\text{Rouse}}$ and $A = 16$, so that $p_{\text{acc}} = 1/e$ when $t/\tau_{\text{anneal}} = 1/4$ for $\Delta L = +1$. The results reported in Table I did not change significantly when τ_{anneal} was increased and A was varied between 10–20. Most of the moves that obey topological restrictions are accepted at first, and as the system cools, the contours of the chains collapse onto their primitive paths.

Finally, to generate a statistical distribution of primitive paths, we adopt the following ''regrowing'' procedure. From the box containing the primitive paths, we select a chain at random and delete it. Choosing one of its two ends randomly, we ''grow'' a new chain in its place subject to the constraints of excluded volume (both intramolecular and intermolecular), chain connectivity, and chain uncrossability. We compute its primitive-path length, record it, and

TABLE I. Simulations of N_p polymer chains with N beads each were carried out in a cubic simulation box of length L_{box} with periodic boundary conditions. After equilibration the mean contour length L_0 and mean-squared end-to-end displacement $\langle R^2 \rangle$ were computed. L_{pp} is the mean primitive-path length of the equilibrated melt computed using the method described in [18]. $L_{pp}/\sqrt{\langle R^2 \rangle} = 0.82$ for unentangled chains. All distances are in units of lattice spacing.

N	N_p	L_{box}	L_0	$\langle R^2 \rangle$	L_{pp}	L_{eq}[a]	$L_{pp}/\sqrt{\langle R^2 \rangle}$
10	400	20	12.6 ± 0.03	20.2 ± 0.56	5.0 ± 0.08	···	1.11 ± 0.02
32	125	20	43.9 ± 0.12	74.4 ± 4.97	11.1 ± 0.40	···	1.29 ± 0.06
75	180	30	104.4 ± 0.18	180.0 ± 10.84	22.7 ± 0.55	···	1.69 ± 0.07
125[b]	364	45	174.4 ± 0.14	337.2 ± 14.65	37.9 ± 0.57	34.5	2.06 ± 0.05
300	277	55	421.2 ± 0.24	732.6 ± 36.90	86.5 ± 1.01	76.0	3.20 ± 0.09
500	216	60	702.7 ± 0.41	1189.2 ± 69.67	141.7 ± 1.52	122.5	4.11 ± 0.13

[a]Standard error of the mean is of the order of 0.0001.
[b]Equilibrating this system required about 1.5 days and annealing it to obtain L_{pp} required about 3 h. Regrowing and deleting the chains 10^6 times to compute L_{eq} took about two weeks on a single 1 GHz Pentium 3 processor.

then restore the originally deleted chain. Note that there is plenty of space to regrow the chain, since the primitive paths occupy only a small fraction ($\sim 20\%$) of the sites on the lattice taken by the original chains. We repeated this process of deleting, regrowing, recording, and restoring until we amassed good statistics.

Results.—We were able to reproduce all the results reported by Shaffer [15]. We obtained $\langle R^2\rangle \sim (N-1)^{1.02\pm0.03}$, which reflects the Gaussian character of the chains in the system, and an average characteristic ratio $C_\infty = 1.17$, where $\langle R^2\rangle = C_\infty\langle b^2\rangle(N-1)$, $\langle b^2\rangle$ being the mean-squared bond length. For the BFM, $\langle b^2\rangle \approx 2.04$.

In an unentangled melt, the primitive-path length is simply the end-to-end distance, which has a distribution

$$\psi(R) = 4\pi R^2\left(\frac{\beta}{\sqrt{\pi}}\right)^3 \exp(-\beta^2 R^2), \tag{2}$$

where $\beta^2 = 1.5/\langle R^2\rangle$. The distribution ψ has a maxima at $1/\beta \approx 0.82\sqrt{\langle R^2\rangle}$. In entangled systems, the primitive path becomes tortuous and longer as it navigates around topological obstacles. Thus, the ratio $L_{pp}/\sqrt{\langle R^2\rangle}$ increases beyond 0.82 as the number of the entanglements increases (see Table I).

From the ensemble of primitive paths, we calculate the mean primitive-path step length $a \equiv \langle R^2\rangle/L_{pp}$, which corresponds to the mean distance between entanglements, and the average number of bonds per entanglement distance $N_e \equiv (N-1)a^2/\langle R^2\rangle$. Since the BFM is a lattice-based model, the primitive path is forced to ''snap on'' to the edges of the cells constituting the lattice. The coarse-grained nature of the lattice implies that values of L_{pp} in continuous space would be somewhat smaller.

As chains get longer and more entangled, a and N_e increase and saturate to constant values (Fig. 1) values. Using data for $N \geq 125$, the mean value of $a = 8.59$, which is about five times longer than the Kuhn step and is reasonable for an entangled melt. Similarly, the average value of $N_e = 29.32$ is consistent with the value inferred by Shaffer [15] using a different method of calculation.

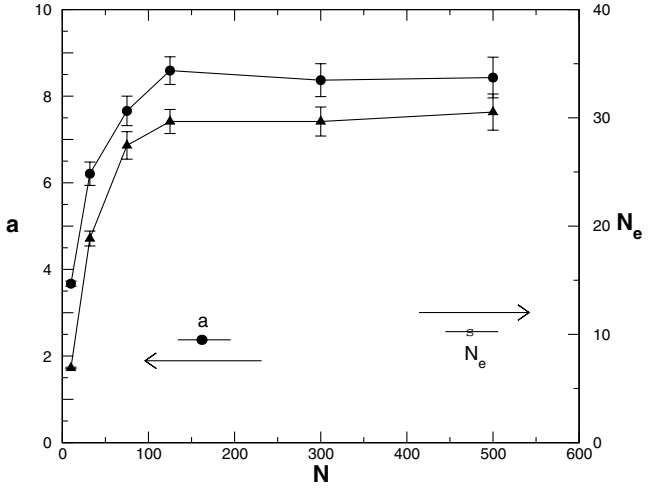

FIG. 1. Primitive-path step length a (filled circles, on the left y axis) and the number of monomers per primitive-path step N_e (filled triangles, on the right y axis), as a function of chain length.

The entropic potential can be derived from the distribution of primitive-path lengths $U(L) = -TS(L) \sim -k_B T \ln\psi(L)$. Thus,

$$\frac{U(L) - U(L_{\rm eq})}{k_B T} = \ln\frac{\psi(L_{\rm eq})}{\psi(L)} \tag{3}$$

In Fig. 2 we plot $[U(L) - U(L = L_{\rm eq})]/Z_{\rm eq}$ obtained from the simulations via Eq. (3), where $Z_{\rm eq} = L_{\rm eq}/a_{\rm eq}$. We find $a_{\rm eq} = \langle R^2\rangle/L_{\rm eq} = 9.72$ (see discussion below). Thus, $N = 125$, 300, and 500, correspond to $Z_{\rm eq} = 3.5$, 7.9, and 12.5 entanglements, respectively. To assess the viability of the quadratic power law for the potential we fit the data to Eq. (1) using ν as a fitting parameter. Figure 2 shows that the entropic potential indeed has a quadratic form, even for substantially deep fluctuations. The values of ν regressed were 1.49 ± 0.08, 1.37 ± 0.02, and 1.36 ± 0.04, for $N = 125$, 300, and 500, respectively. This is in fair agreement with the value of $\nu = 1.5$ derived by [1].

Discussion.—As reported in Table I, the average primitive-path length of the chains, L_{pp} is systematically larger, by about 10%, than $L_{\rm eq}$, the average primitive-path length obtained during the regrowing phase. This occurs because the regrowing phase is carried out in a matrix of

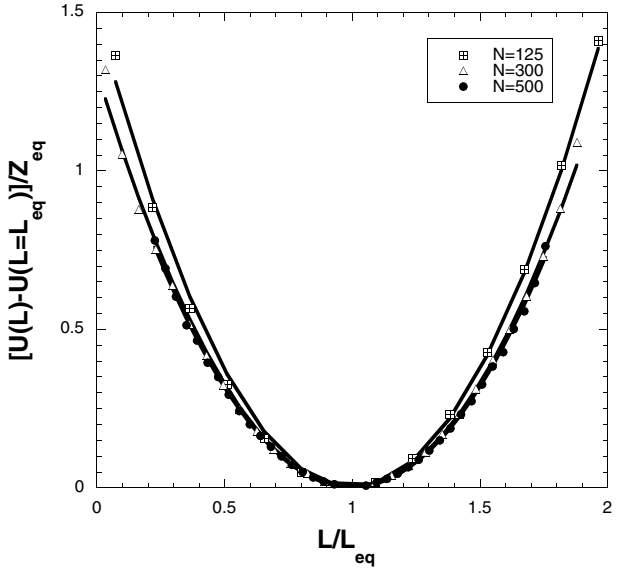

FIG. 2. Symbols are simulation results for $N = 125$ ($Z_{\rm eq} = 3.5$ entanglements), $N = 300$ ($Z_{\rm eq} = 7.9$ entanglements), and $N = 500$ ($Z_{\rm eq} = 12.5$ entanglements). Lines are best fits using Eq. (1) with ν as a fitting parameter. The values of ν regressed were 1.49 ± 0.08, 1.37 ± 0.02, and 1.36 ± 0.04, for $N = 125$, 300, and 500, respectively.

primitive paths whose slack has been completely roped in. Thus, the chain being regrown cannot entangle with unreeled loops as occurs in the original ensemble of chains before the slack has been reeled in. The discrepancy between L_{eq} and L_{pp} (and therefore, between a_{eq} and a) brings to light a possible ambiguity in definition and calculation of a primitive path.

We introduced the process of regrowing the chain because Eq. (1) was originally derived in a fixed matrix of primitive chains and also to obtain better statistics. For example, to obtain the simulation data reported in Fig. 2, we repeated the process of regrowing, 10^6 times for $N = 125$ and 300, and 3.1×10^6 times for $N = 500$. In principle, we could obtain the same statistics by using ensembles with a large number ($\sim 10^6$, say) of chains. However, the process of equilibrating and annealing the whole ensemble simultaneously is computationally much more expensive than annealing a randomly selected chain from the frozen matrix 10^6 times.

Conclusion.—We employed the BFM to examine the applicability of the entropic potential that forms the underlying basis for rheological theories of branched polymer melts. Contrary to previous lattice-based calculations, our simulations confirm the quadratic functionality of Eq, (1), for both shallow and deep flucutations. The value of the prefactor ν is comparable with the theoretical estimate of 1.5. To determine its value more precisely, off-lattice MD simulations should be carried out.

This material is based upon work supported by the National Science Foundation under Grant No. DMR 0305437. Any opinions expressed are those of the authors, not of the NSF. The authors would like to thank Qiang Zhou for helpful discussions.

*Electronic address: rlarson@umich.edu

[1] M. Doi and N. Kuzuu, J. Polym. Sci., Polym. Lett. Ed. **18**, 775 (1980).
[2] D. Pearson and E. Helfand, Macromolecules **17**, 888 (1984).
[3] T. McLeish, Adv. Phys. **51**, 1379 (2002).
[4] M. Doi and S. F. Edwards, *The Theory of Polymer Dynamics* (Clarendon Press, Oxford, 1988).
[5] E. Helfand and D. Pearson, J. Polym. Sci., Polym. Symp. **73**, 71 (1985).
[6] A. Khokhlov and S. Nechaev, Phys. Lett. A **112**, 156 (1985).
[7] M. Rubinstein and E. Helfand, J. Chem. Phys. **82**, 2477 (1985).
[8] E. Zheligovskaya, F. Ternovskii, and A. Khokhlov, Theor. Math. Phys. (Engl. Transl.) **75**, 644 (1988).
[9] E. Helfand and D. Pearson, J. Chem. Phys. **79**, 2054 (1983).
[10] S. Nechaev, A. Semenov, and M. Koleva, Physica A (Amsterdam) **140**, 506 (1986).
[11] R. Ball and T. Mcleish, Macromolecules **22**, 1911 (1989).
[12] S. Milner and T. McLeish, Macromolecules **30**, 2159 (1997).
[13] S. Milner and T. McLeish, Macromolecules **31**, 7479 (1998).
[14] I. Carmesin and K. Kremer, Macromolecules **21**, 2819 (1988).
[15] J. Shaffer, J. Chem. Phys. **101**, 4205 (1994).
[16] J. Shaffer, J. Chem. Phys. **103**, 761 (1995).
[17] S. Brown and G. Szamel, Macromol. Theory Simul. **9**, 14 (2000).
[18] R. Everaers, S. Sukumaran, G. Grest, C. Svaneborg, A. Sivasubramanian, and K. Kremer, Science **303**, 823 (2004).
[19] W. Paul, K. Binder, D. Heermann, and K. Kremer, J. Chem. Phys. **95**, 7726 (1991).
[20] M. Mantina and J. Luettmer-Strathmann, *APS Meeting Abstracts* (American Physical Society, 2003), Abstract No. R1.1114.